Turnitin-IJNEAM2021021

by Nani Djohan1*, Budi Harsono1, Johansah Liman1, Hen Nani Djohan1*, Budi Harsono1, Johansah Liman1, Hen

Submission date: 31-Mar-2021 09:06AM (UTC+0800)
Submission ID: 1546827532
File name: IJNEAM2021021.docx (360.2K)
Word count: 3331
Character count: 17650

International Journal of Nanoelectronics and Materials

Structural, Optical Properties and Raman Spectroscopy of In_2O_3 Doped $LiTaO_3$ Thin Films

Nani Djohan[1*], Budi Harsono[1], Johansah Liman[1], Hendradi Hardhienata[2] and Irzaman[2*]

1 Department of Electrical Engineering, Faculty of Engineering and Computer Science, Universitas Kristen Krida Wacana, Jl. Tj. Duren Raya No. 4, Jakarta 11470, Indonesia

2 Department of Physics, Faculty of Mathematics and Natural Sciences, Bogor Agricultural University, Jl. Raya Dramaga, Bogor 16680, Indonesia

ABSTRACT

In this experiment, undoped, 2 wt.%, 4 wt.% and 6 wt.% In_2O_3 doped $LiTaO_3$ thin films were successfully prepared using the Chemical Solution Deposition (CSD) method with the spin coating technique. The films were grown on the p-type Si (100) substrates with 2 M in 2-methoxyethanol precursor, whose solubility was twisted at 4000 rpm for 30 seconds. Crystalline formation of the films was carried out at annealing temperature 850 ^oC, held for 15 hours with temperature increment speed 1.67 ^{o} C/min. The structural properties of the films were carried out using the XRD device with the interval of 2 theta angles from 20 to 80 degrees with a 0.02 degrees step, where thin films have formed crystals at specific angular peaks with hexagonal-shaped crystal structures. The optical properties and Raman spectra of the films were then obtained using UV-Vis spectrometer and Raman spectroscopy. From the XRD measurement, the result shows a hexagonal crystal structure with lattice parameters a = 5.032-5.051 Å and c = 13.643-13.676 Å, and from the UV-Vis data, we observed that the films have a 5.034-5.184 Ev energy gap with 1.70364373 – 1.70364377 refractive index. Raman analysis produces peaks of $LiTaO_3$, A_1TO_{10} (In_2O_3) and A_1LO_{10} (In_2O_3). Based on the characterization results, we can conclude that the $LiTaO_3$ thin films have the potential to be applied as a light sensor.

Keywords: $LiTaO_3$, In_2O_3, x-ray diffraction, Raman spectroscopy, uv-vis spectroscopy.

1. INTRODUCTION

A thin film made from Lithium tantalate ($LiTaO_3$) is an essential optical material, mainly due to its excellent electro/acousto-optical properties, high pyroelectric coefficient, high curie temperature, small relative dielectric constant, and good consistency of special response. The thickness of the sensitive cells is inversely proportional to the voltage response and detectivity of the detectors [1-3]. Thin layer of material whose thickness is between 10^{-9} m and 10^{-6} m, because of its limited thickness, the bulk material is not suitable for high-performance detection system applications[1,4]. However, $LiTaO_3$ is very attractive and promising [1,5].

There are various kinds of technology to synthesize $LiTaO_3$ thin films. X-ray Diffraction (XRD) technology is based on diffraction of X-Ray when scattering light with a wavelength passing through a crystal lattice with a distance between crystal fields. Data obtained from XRD characterization method is scattering angle (Bragg angle) to intensity. Based on diffraction theory, the diffraction angle depends on the gap of the lattice width, thus affecting the diffraction pattern. In contrast, the diffraction light intensity depends on the number of crystal lattices having the same orientation. Crystal system, parameter of the lattice, the degree of crystallinity, structure type, and orientation can be determined by this method. $LiTaO_3$ thin film with high purity and best intensity could be selected from the XRD measurement [1,6,7].

* nani.djohan@ukrida.ac.id

* irzaman@apps.ipb.ac.id

Solid-state and molecule vibrational properties can be analyzed by using Raman sepctroscopy [8,9]; thus, strain [9,12], doping [9,13,14], stoichiometry [9,10,11] and crystallinity property information can be obtained by this technology. However, Raman spectroscopy is very sensitive to minor modifications made in the lithium tantalate compound structure, such as some frequency shifts, damping of optical phonons, or even the appearance of new lines [15]. Density functional theory (DFT) is the combination of Raman with theoretical approaches yielding phonon eigenvectors [9]. In this experiment, four types of solution ($LiTaO_3$, $LiTaO_3$ + 2 wt.% In_2O_3, $LiTaO_3$ + 4 wt.% In_2O_3, and $LiTaO_3$ + 6 wt.% In_2O_3) were produced by mixing and dissolving different molar ratios of chemical powders in the 2-methoxyethanol solvent. The films were then grown on the p-type silicon substrates utilizing spin coater and annealed at 850°C temperature. The structural and optical properties of the films were then carried out using X-Ray Diffractometer and UV-Vis spectrometer, respectively [6,7,11,16]. Furthermore, Raman spectra were carried out using Raman Spectroscopy to investigate the transversal and longitudinal phonon modes of the films [8,9,15,17-20].

2. MATERIAL AND METHODS

The p-type Si(100) substrates cut in size of 1x1 cm^2 were ultrasonically cleaned in acetone (C_3H_6O) and repeated sequentially using methanol (CH_3OH) and deionized water successively for 15 minutes [3,6,21-24]. The undoped $LiTaO_3$ solution was prepared by dissolving 0.5897 gram of lithium tantalate (≥99.99%, Sigma-Aldrich 704393-5G) in 2.5 ml of 2-methoxyethanol. The 2 wt.%, 4 wt.%, and 6 wt.% In_2O_3 doped $LiTaO_3$ solutions were prepared by dissolved 0.5897 gram of lithium tantalate and 0.01179 gram, 0.0236 gram, and 0.03538 gram of indium(III) oxide (99.99%, Sigma-Aldrich 289418-10G), respectively in 2.5 ml of 2-methoxyetanol.
To get the homogeneous $LiTaO_3$ solutions, the solutions were stirred using Vortex 3000 mixer and then sonicated using an ultrasonicator device (J.P Selecta) for 30 minutes [3,6]. Furthermore, the thin films were deposited on the p-type Si (100) substrates using spin coater for 30 seconds using a rotating speed of 4000 rpm. This process was repeated three times with a one-minute time interval [3,4,6,16,21-26]. The annealing process was done using Nabertherm B410 furnace at temperature 850°C for 15 hours, with a temperature increment speed of 1.67°C/min. The structural properties of the thin-film crystal were then obtained with an X-Ray Diffractometer (Bruker D2 PHASER). Furthermore, the thin films were characterized by using a UV-Vis spectrometer (Ocean Optics USB4000-UV-Vis) and Raman spectroscopy (Horriba iHR550).

3. RESULTS AND DISCUSSION

3.1 Structural properties

The XRD patterns of $LiTaO_3$ thin films were determined from $20^o \leq 2\theta \leq 80^o$ intervals with a scanning rate of 0.02°/minute [6,11,27-29]. Figure 1 shows the XRD patterns of undoped and In_2O_3 doped $LiTaO_3$ thin films [6,11,27]. The Miller index values were assigned by reffering to the standard x-ray diffraction powder patterns file (JCPDS Natl Bur, 1977) and were in good agreement with the values reported in the file. The XRD patterns showed that $LiTaO_3$ thin films were both amorphous and crystalline with hexagonal crystal structure. All the XRD patterns showed a preferred strong peak at (012) diffraction plane. The peaks profiles of the two most dominant peaks at (012) and (104) diffraction plane was obtained by Gaussian fitting. Peak position (2θ) and the full width at half maximum (FWHM) from the peaks are shown in Table 1.

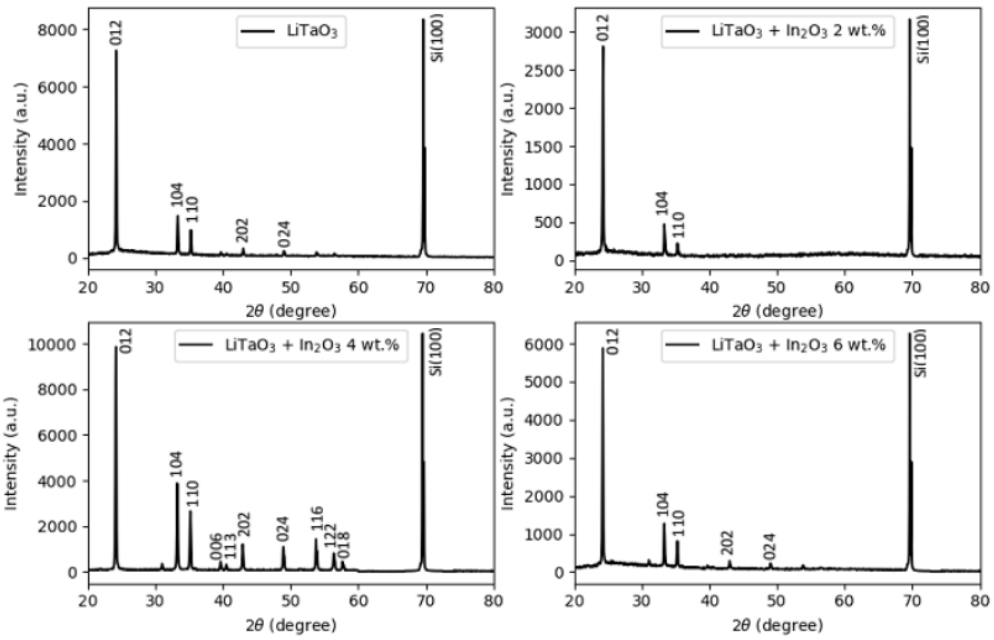

Figure 1. XRD patterns of $LiTaO_3$ thin films with different doped In_2O_3 at annealing temperature 850°C.

The crystallite size (D) of the undoped and In_2O_3 doped $LiTaO_3$ thin films was calculated using Debye Scherer's formula.

$$D = \frac{k\lambda}{\beta cos\theta} \quad (1)$$

Where k is the shape factor (= 0.9), λ is the X-ray radiation wavelength (= 0.15406 nm), β is FWHM of diffraction peak in radian, and θ is the Bragg's diffraction angle in radian. The highest crystallite size values observed were 51.408 nm and 46.620 nm for (012) and (104) diffraction plane in 6 wt.% In_2O_3 doped $LiTaO_3$ thin film. The crystallite size decreased in line with the decrease in doping concentration, as shown in Table 1.

The dislocation density (δ) of the undoped and In_2O_3 doped $LiTaO_3$ thin films could be obtained using the Williamson-Smallman formula.

$$\delta = \frac{1}{D^2} \quad (2)$$

Where D is the crystallite size of the films obtained from Eq.1, it was observed that the dislocation density decreases as doping concentration increases.

The lattice strain (ε) of the undoped and In_2O_3 doped $LiTaO_3$ thin films was calculated by using the following formula.

$$\varepsilon = \frac{\beta}{4\tan\theta} \quad (3)$$

The data show that when doping concentration increases beyond 2 wt.%, lattice strain will decrease. This suggests the creation of fewer defects in the $LiTaO_3$ lattice. All the calculated results from the XRD data are shown in Table 1.

The interplanar spacing (d_{hkl}) for each peak can be calculated using Bragg's formula, as shown in Eq. 4. The lattice parameters (a and c) can be calculated from the interplanar spacing equation for hexagonal lattice as shown in Eq. 5, where hkl is the Miller indices of the plane of diffraction.

$$d_{hkl} = \frac{\lambda}{2sin\theta} \quad (4)$$

$$\frac{1}{d_{hkl^2}} = \frac{4}{3}\left(\frac{h^2+hk+k^2}{a^2}\right) + \frac{l^2}{c^2} \quad (5)$$

The calculated lattice parameters for undoped and various wt.% In_2O_3 doped $LiTaO_3$ thin films are tabulated in Table 2. From the data in table 2, the calculated lattice parameters were slightly different from the JCPDS data due to differences in annealing temperature.

Table 1 Crystallite size, dislocation density, and lattice strain of $LiTaO_3$ thin films doped with In_2O_3

Sample	Diffraction plane	2θ (deg)	FWHM (deg)	Crystallite size (nm)	Dislocation density (cm^{-2}) x 10^{10}	Lattice strain x 10^{-3}
$LiTaO_3$	0 1 2	24.186	0.160	50.805	3.874	3.257
	1 0 4	33.293	0.197	42.001	5.669	2.881
$LiTaO_3$ + 2 wt.% In_2O_3	0 1 2	24.217	0.167	48.638	4.227	3.398
	1 0 4	33.333	0.197	42.016	5.665	2.877
$LiTaO_3$ + 4 wt.% In_2O_3	0 1 2	24.131	0.160	50.685	3.893	3.272
	1 0 4	33.231	0.189	43.834	5.204	2.765
$LiTaO_3$ + 6 wt.% In_2O_3	0 1 2	24.187	0.158	51.408	3.784	3.218
	1 0 4	33.293	0.178	46.620	4.601	2.596

Table 2 Lattice parameter values of $LiTaO_3$ thin films doped with In_2O_3 hexagonal structure

Lattice parameter	$LiTaO_3$	$LiTaO_3$ + 2 wt.% In_2O_3	$LiTaO_3$ + 4 wt.% In_2O_3	$LiTaO_3$ + 6 wt.% In_2O_3	JCPDS (Natl Bur, 1977)
c (Å)	13.658	13.643	13.676	13.658	13.755
a (Å)	5.038	5.032	5.051	5.038	5.153

3.2 Optical properties

The optical properties of the undoped and In_2O_3 doped $LiTaO_3$ thin films were investigated by analyzing the reflectance spectra in the wavelength between 230 nm and 850 nm (UV-Vis range). The reflectance spectra of the synthesized films are shown in figure 2. In the reflectance spectra, we observed that the films have low reflectance in the ultra-violet range and high reflectance in the visible range. We could estimate the band gap energy (Eg) values of the synthesized films from the reflectance spectra. The recorded reflectance spectra were first transformed to the absorption spectra by applying the Kubelka-Munk function (F(R)). Then the Tauc plot method is employed to determine the band gap energy[3,6,32]. The Kubelka-Munk function and the Tauc formula are given in Eq.6 dan Eq.7, respectively.

$$F(R) = \frac{K}{S} = \frac{(1-R)^2}{2R} \propto \alpha_{K-M} \quad (6)$$

$$(\alpha_{K-M}hv)^{1/n} = B(hv - Eg) \quad (7)$$

K and S are absorption and scattering coefficients, respectively. R is reflectance value, hv is the photon's energy, B is a constant, Eg is the band gap energy, and n is the nature of the electron transition (= ½ for direct transition band gap).

From the Tauc plot, it is found that the optical band gap energy of undoped, 2 wt.%, 4 wt.%, and 6 wt.% In_2O_3 doped $LiTaO_3$ thin films are 5,034 eV, 5,079 eV, 5.122 eV, and 5,184 eV, respectively, as shown in figure 3. From the data, it was observed that the increase in doping concentration also increased the band gap energy of the films.

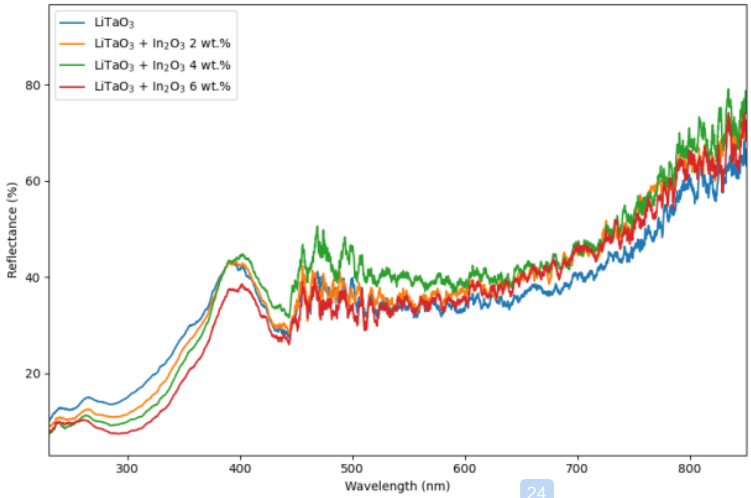

Figure 2. Reflectance spectra of $LiTaO_3$ thin films.

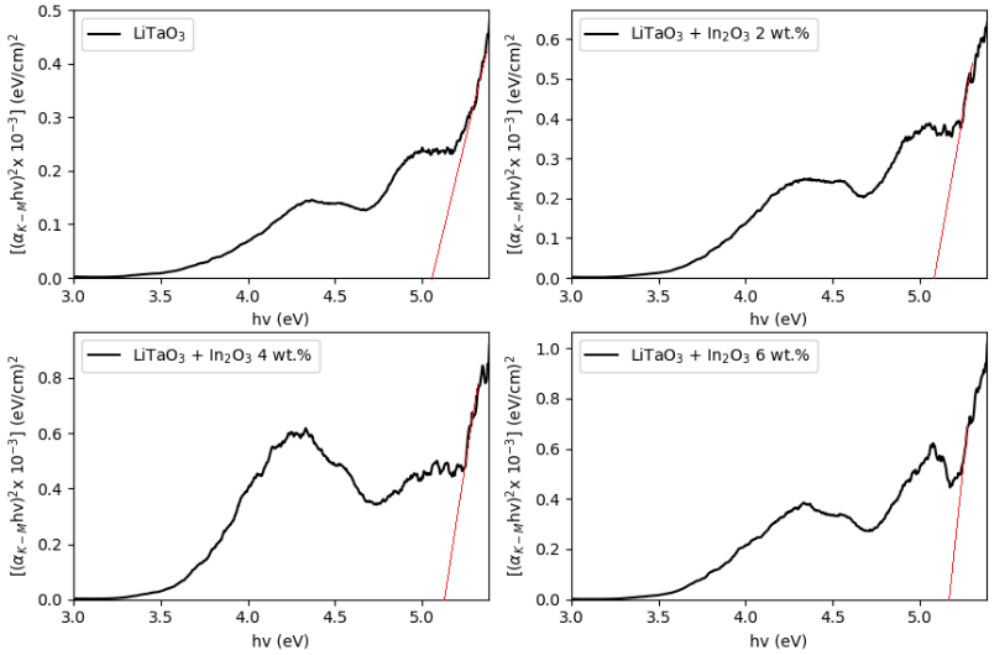

Figure 3. Energy band gap of $LiTaO_3$ thin films.

Refractive index (n_e) of the films were obtained by using Sellmeier formula[6,33,34].

$$n_e^2(\lambda,T) = A + \frac{B+b(T)}{\lambda^2-[C+c(T)]^2} + \frac{E}{\lambda^2-F^2} + \frac{G}{\lambda^2-H^2} + D\lambda^2 \quad (8)$$

Where λ is the wavelength related to the band gap energy value, b(T), c(T) is the temperature dependent, and A,B,C,D,E,F,G,H is the coefficients of Sellmeier. The data show that the value of the refractive index also increase as the band gap energy incresed. The refractive index, band gap energy and related color spectra of undoped, 2 wt.%, 4 wt.%, and 6 wt.% In_2O_3 doped $LiTaO_3$ thin films were listed in Table 3.

Table 3 The energy gap and the refractive index of $LiTaO_3$ thin films

Sample	Band gap (eV)	Wavelength (nm)	Color spectra	Refractive index
LiTaO3	5.034	246.855	ultraviolet	1.70364373
LiTaO3 + 2 wt.% In2O3	5.079	244.692	ultraviolet	1.70364374
LiTaO3 + 4 wt.% In2O3	5.122	242.529	ultraviolet	1.70364375
LiTaO3 + 6 wt.% In2O3	5.184	239.715	ultraviolet	1.70364377

3.3 Raman Spectrum

Raman spectroscopy technology can be used to mapping demonstrates a spatial variation of the widths of the phonon bands for stoichiometric, congruent, and quasicongruent samples. To investigate the compositional uniformity of these crystals, we use Raman spectra of $LiTaO_3$ single crystals with various stoichiometric [8,9,15]. The first principles, the peaks of Raman intensity were assigned by reffering to the mode energy [9,30,31]. The phonons identification may become complicated because some Raman intensity might be lost on the calculated modes [9]. Longitudinal phonon mode was observed when polarization vectors and phonon wave vector are parallel, whereas transversal phonon mode was observed when polarization vectors and phonon wave vector are perpendiculars.

Figure 4 shows the Raman spectrum of undoped, 2 wt.%, 4 wt.%, and 6wt.% In_2O_3 doped $LiTaO_3$ thin films. In this experiment, Raman spectra were obtained by Raman spectroscopy in the range from 100 to 1000 cm^{-1}.

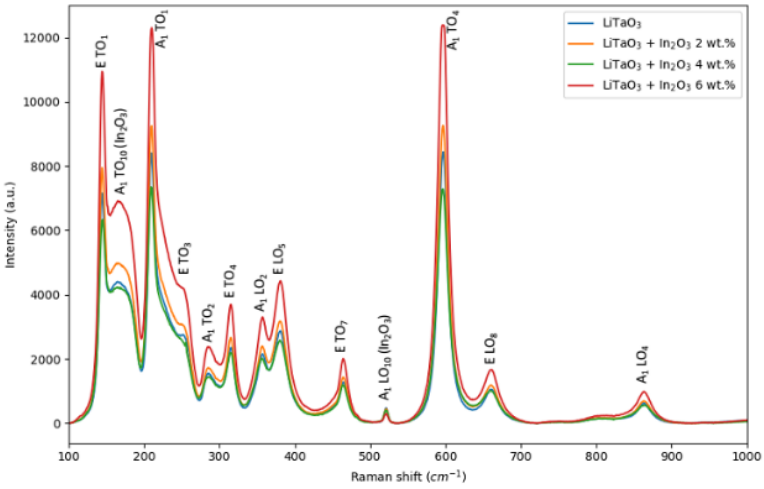

Figure 4. Raman spectroscopy of $LiTaO_3$.

Table 4 shows the result of active phonon frequencies of undoped, 2%, 4%, and 6% In_2O_3 doped $LiTaO_3$ thin films. The experiment results show that the most significant deviation is 5 cm^{-1} at A_1 TO_4 and the mean deviation is 1.82 cm^{-1}.

Table 4 Theory and experiment result of active phonon frequencies of $LiTaO_3$

Symmetry	Mode	Exp.	Literature [9]	Mode	Exp.	Literature [9]
A1	TO1	209	209	LO1		255
A1	TO2	285	286	LO2	356	355
A1	TO3		376	LO3		403
A1	TO4	596	591	LO4	863	866
E	TO1	144	144	LO1		190
E	TO2		199	LO2		
E	TO3	253	253	LO3		279
E	TO4	315	319	LO4		
E	TO5		409	LO5	380	381
E	TO6		420	LO6		453
E	TO7	463	459	LO7		
E	TO8		590	LO8	661	660
E	TO9		669	LO9		866
A1	TO10	165		LO10	521	

Phonon activities in hexagonal crystal structures (XRD analysis) and electron jump from valence band into induction band to become free electron (UV-Vis analysis) leads to the occurrence of transversal and longitudinal mode (Raman spectroscopy) and electron free radicals on the thin film surface. The intensity difference of the free radicals shown in Raman spectroscopy (Figure 4) is caused by In^{3+} doping and radius in the $LiTaO_3$ thin films.

4. CONCLUSION

The making of In_2O_3 doped $LiTaO_3$ thin films with CSD method was succeeded. Analysis of the thin films was conducted using XRD, UV-Vis spectrometer and Raman spectroscopy. Based on the characterization result, we can be concluded that the $LiTaO_3$ thin films have the potential to be applied as a light sensor, especially in the ultraviolet region.

ACKNOWLEDGEMENTS

This study was supported by the Ministry of Research, Technology and Higher Education of the Republic of Indonesia through the Research Grant No. 004/AKM/MONOPNT/2019.

REFERENCES

[1] Gou J, Wang J, Huang Z. H and Jiang Y. D 2013 *Key Eng. Mater.* 531-532446.

[2] V. Norkus: *Proceedings of SPIE*, Vol. 5251 (2004), p. 121.

[3] N Djohan, R Estrada, N Sevani, H Hardhienata, Irzaman: The Optical Band Gap Based on K-M Function on layer of $LiTaO_3$ with Variation Treatment of Annealing Temperature, ICSGTEIS 2018, October 2018.

[4] R Estrada, N Djohan, D Pasole, M Dahrul, A Kurniawan, J Iskandar, H Hardhienata, and Irzaman: The optical band gap of $LiTaO_3$ and Nb_2O_5 – doped $LiTaO_3$ thin films based on Tauc Plot method to be applied on satellite, *IOP Conf. Ser.: Earth Environ. Sci.,* Vol 54 (1), No. article 012092, February 2017.

[5] D. Y. Zhang, D. G. Huang, J. H. Li, K. Li, D. D. Dan and Z. Dong: *Journal of Infrared and Millimeter Waves,* Vol. 26 (2007) No. 3, p. 170 (In Chinese).

[6] N Djohan, R Estrada, N Sevani, H Hardhienata and Irzaman: Crystalline Structure and optical properties of thin film $LiTaO_3$, *IOP Conf Ser.: Earth Environ.*Sci. 284012039, 2019.

[7] Fakhri M A, Douri Y A, Hashim U, Salim E T 2016 *Adv. Mater. Res.* 1133457.

[8] S. M. Kastritskii, M. Aillerie, P. Bourson, D. Kip: Raman Spectroscopy study of compositional in homogeneity in lithium tantalate crystals *Applied Physics B* (2009) 95: 125-130.

[9] S. Sanna, S. Neufeld, M. Rűsing, G. Berth, A. Zrenner, and W. G. Schmidt: Raman scattering efficiency in $LiTaO_3$ and $LiNbO_3$ crystals *Physical Review B 91, 224302* (2015).

[10] E. Buixaderas, I. Gregora, M. Savinov, J. Hlinka, L. Jin, D. Damjanovic, and B. Malic, *Phys Rev B 91, 014104* (2015).

[11] Irzaman, Y. Pebriyanto, E. R. Apipah, I. Noor, A. Alkadri: Characterization of optical and structural of lanthanum doped $LiTaO_3$ thin films *Integrated Ferroelectrics*. 167, 137-145 (2015).

[12] A. Bartasyte, S. Margueron, J. Kreisel, P. Bourson, O. Chaix-Pluchery, L. Rapenne-Homand, J. Santiso, C. Jimenez, A. Abrutis, F. Weiss, and M. D. Fontana, *Phys Rev B 79, 104104* (2009)

[13] R. Mouras, M. D. Fontana, P. Bourson, and A. V. Postnikov, *J Phys: Condens. Matter* 12, 5053 (2000).

[14] R. Quispe-Siccha, E. V. Mejfa-Uriarte, M. Villagran- Muniz, D. Jaque, J. Garcia Solé, F. Jaque, R. Y. Sato-Berrú, E. Camarillo, J. Hernández A., and H. Murrieta. S., *J Phys: Condens Matter* 21, 145401 (2009).

[15] Y. Repelin, E. Husson, F. Bennani, C. Proust: Raman spectroscopy of lithium niobate and lithium tantalate. Force field calculations. *Journal of Physics and Chemistry of Solids* 60 (1999) 819-825.

[16] N Djohan, R Estrada, D Sari, M Dahrul, A Kurniawan, J Iskandar, H Hardhienata, and Irzaman: The effect of annealing temperature variation on the optical properties test of $LiTaO_3$ thin films based on Tauc Plot method for satellite technology, *IOP Conf. Ser.: Earth Environ. Sci,* Vol. 54(1), No. article 012093, February 2017.

[17] P. S. Zelenovskiy, V. Y. Shur, P. Bourson, M. D. Fontana, D. K. Kuznetsov, and E. A. Mingaliev, *Ferroelectrics* 398, 34 (2010).

[18] M. D. Fontana, R. Hammoum, P. Bourson, S. Margueron, and V. Y. Shur, *Ferroelectrics* 373, 26 (2008).

[19] G. Berth, W. Hahn, V. Wiedemeier, A. Zrenner, S. Sanna, and W. G. Schmidt, *Ferroelectrics* 420, 44 (2011).

[20] S. Sanna, G. Berth, W. Hahn, A. Widhalm, A. Zrenner, and W. G. Schmidt, *Ferroelectrics* 419, 1 (2011).

[21] Irzaman, Siskandar R, Nabilah N, Aminullah, Yuliarto. B, Hamam K. A, and Alatas. H: Application of lithium tantalite ($LiTaO_3$) films as light sensor to monitor the light status in the Arduino uno based energy-saving automatic light prototype and passive infrared sensor. *Ferroelectrics*. 524, 44-55 (2018).

[22] Irzaman, Sitompul H, Masitoh, Misbakhusshudur M, and Mursyidah: Optical and structural properties of lanthanum doped lithium niobate thin films. *Ferroelectrics*. 502, 9-18 (2016).

[23] Irzaman, Siskandar R, Aminullah, Irmansyah, and Alatas H: Characterization of $Ba_{0,55}Sr_{0,45}TiO_3$ film as light and temperature sensors and its implementationon automatic drying system model. *Integrated Ferroelectrics*. 168, 130 (2016).

[24] Irzaman, Putra I R, Aminullah, Syafutra H, Alatas H, 2016 *Procedia Environ*. Sci. 33607.

[25] N Djohan, R Estrada, F. I. W. Sari, A Kurniawan, J Iskandar, M Dahrul, H Hardhienata, and Irzaman: Classification of undoped and 10% Ga_2O_3-doped $LiTaO_3$ thin films based on electrical conductivity and phase characteristic, *ARPN J. Eng. Appl. Sci*., Vol 12 (12), pp. 3779-3782, June 2017.

[26] R. Estrada, N. Djohan, G. C. Rundupadang, A. Kurniawan, I. Iskandar, M Dahrul, H. Hardhienata, Irzaman: Electrical Properties Test of Dielectric Constant and Impedance Characteristic Thin Films of $LiTaO_3$ and 10% Ga_2O_3-doped $LiTaO_3$, *ARPN Journal of Engineering and Applied Sciences.* 12: 3813-3816 (2017).

[27] B. Zielińska, E. Mijowska, R. J. Kalenczuk: Synthesis, characterization and photocatalytic properties of lithium tantalate, *Materials Characterization* 68(2012) 71-76.

[28] A. Kassim, S. Nagalingam, S. M. Ho, and N. Karrim: XRD and AFM studies of ZnS thin films produced by electrodeposition method. *Arabian Journal of Chemistry*. 3, 243-249 (2010).

[29] D. Rajesh and C. S. Sunandana: XRD, optical and AFM studies on pristine and partially iodized Ag thin film. *Result in Physics*. 2, 22-25 (2012).

[30] K. Parlinski, Z. Q. Li, and Y. Kawazoe, *Phys. Rev. B 61, 272* (2000).

[31] V. Casiuc, A. V. Postnikov, and G. Borstel, *Phys. Rev. B 61, 8806* (2000).

[32] Mulyadi, Rika W, Sulidah, Irzaman, Hardhienata H 2017 Barium Strontium Titanate Thin Film Growth with rotational speed variation as a satelite temperature sensor prototype *IOP Conf. Ser.: Earth Environ. Sci.* 54 012094.

[33] Bruner A, Eger D, Oron M B, Blau P, Katz M, Ruschin 2003 Temperature-dependent Sellmeier equation for the refractive index of stoichiometric lithium tantalate *Opt. Lett. 28 194.*

[34] Weng W -L, Liu Y -W, Zhang X -Q 2008 Temperature-dependent Sellmeier Equation for 1.0 mol % Mg-Doped Stoichiometric Lithium Tantalate *Chin. Lett. 25 4303.*

Turnitin-IJNEAM2021021

ORIGINALITY REPORT

23%	16%	21%	5%
SIMILARITY INDEX	INTERNET SOURCES	PUBLICATIONS	STUDENT PAPERS

PRIMARY SOURCES

1	www.electric-material.com Internet Source	2%
2	Submitted to Institut Pertanian Bogor Student Paper	2%
3	iopscience.iop.org Internet Source	1%
4	Endah K. Palupi, Husin Alatas, Irzaman, Yaya Suryana, Arga Aridarma, Rofiqul Umam, Bibin B. Andriana, Hidetoshi Sato. "Optimization of optical properties of Ba0.2Sr0.8TiO3 thin films for a glucose sensor implementation", Biomedical Spectroscopy and Imaging, 2020 Publication	1%
5	"Advanced Nanomaterials and Nanotechnology", Springer Science and Business Media LLC, 2013 Publication	1%
6	De-Long Zhang. "Raman scattering study on formation of ErNbO4 powder", physica status solidi (a), 08/2004	1%

Publication

7	Gou, Jun, Jun Wang, Ze Hua Huang, and Ya Dong Jiang. "Preparation of $LiTaO_3$ Nano-Crystalline Films by Sol-Gel Process", Key Engineering Materials, 2012. Publication	1%
8	www.iept.tu-clausthal.de Internet Source	1%
9	Monica Popa, Masato Kakihana. "Ultrafine niobate ceramic powders in the system RExLi1−xNbO3 (RE: La, Pr, Sm, Er) synthesized by polymerizable complex method", Catalysis Today, 2003 Publication	1%
10	N Djohan, R Estrada, N Sevani, H Hardhienata, Irzaman. " Crystalline structure and optical properties of thin film LiTaO ", IOP Conference Series: Earth and Environmental Science, 2019 Publication	1%
11	koreascience.or.kr Internet Source	1%
12	www.intechopen.com Internet Source	1%
13	Jitesh Agrawal, Tejendra Dixit, Palani I A, M S Ramachandra Rao, Vipul Singh. "Fabrication of high responsivity deep UV photo-detector based	1%

on Na doped ZnO nanocolumns", Journal of Physics D: Applied Physics, 2018
Publication

14	worldwidescience.org Internet Source	1%
15	Submitted to RMIT University Student Paper	1%
16	Submitted to University of St Andrews Student Paper	1%
17	Oleksandr L. Stroyuk, Natalia I. Ermokhina, Ganna V. Korzhak, Natalya S. Andryushina et al. "Photocatalytic and photoelectrochemical properties of hierarchical mesoporous TiO2 microspheres produced using a crown template", Journal of Photochemistry and Photobiology A: Chemistry, 2017 Publication	<1%
18	link.springer.com Internet Source	<1%
19	pubs.rsc.org Internet Source	<1%
20	res.mdpi.com Internet Source	<1%
21	John Schmidt. "Light-Induced Yellowing of Mechanical and Ultra-High Yield Pulps. I. Effect	<1%

of Methylation, NaBH4, Reduction and Ascorbic Acid on Chromophore Formation", Journal of Wood Chemistry and Technology, 12/1/1991
Publication

22	S. Prucnal, Jiada Wu, Y. Berencén, M. O. Liedke, A. Wagner, F. Liu, M. Wang, L. Rebohle, S. Zhou, Hua Cai, W. Skorupa. "Engineering of optical and electrical properties of ZnO by non-equilibrium thermal processing: The role of zinc interstitials and zinc vacancies", Journal of Applied Physics, 2017 Publication	<1%
23	shura.shu.ac.uk Internet Source	<1%
24	hal.archives-ouvertes.fr Internet Source	<1%
25	aip.scitation.org Internet Source	<1%
26	onlinelibrary.wiley.com Internet Source	<1%
27	www.nuigalway.ie Internet Source	<1%
28	Mulyadi, Rika Wahyuni, Hendradi Hardhienata, Irzaman. "Barium strontium titanate thin film growth with variation of lanthanum dopant compatibility as sensor prototype in the satellite	<1%

technology", IOP Conference Series: Earth and Environmental Science, 2018
Publication

29	nanoscalereslett.springeropen.com Internet Source	<1%
30	physik.uni-paderborn.de Internet Source	<1%
31	www.hindawi.com Internet Source	<1%
32	www.tandfonline.com Internet Source	<1%
33	Aneer Lamichhane, Nuggehalli M. Ravindra. "Energy Gap-Refractive Index Relations in Perovskites", Materials, 2020 Publication	<1%
34	K. Chaitanya Kumar, S. Kaleemulla. "Effect of Ni incorporation on structural, optical and magnetic properties of electron beam evaporated ZnS thin films", Journal of Physics and Chemistry of Solids, 2019 Publication	<1%
35	binwei sun, Jun Wang, Jun Gou, Xianchao Liu, Yadong Jiang. "Influence of thermal annealing on structural and optical properties of RF-sputtered LiTaO3 thin films", Materials Research Express, 2018	<1%

Publication

Exclude quotes	Off	Exclude matches	Off
Exclude bibliography	On		

Turnitin-IJNEAM2021021

GRADEMARK REPORT

FINAL GRADE

/0

GENERAL COMMENTS

Instructor

PAGE 1

PAGE 2

PAGE 3

PAGE 4

PAGE 5

PAGE 6

PAGE 7

PAGE 8

PAGE 9